Materials Horizons

Accepted Manuscript

Conceptual Insights

The biomimetic design principles delineated herein—creation of shell-mimicking assembly constituting compact rigid phase and ordered tenacious filaments—are extended to make a new type of polymer composites, which are composed of well-aligned multiscale inorganic rigid fillers, highly oriented polymer crystals (i.e., the so-called classic shish-kebab and hybrid shish-kebab crystals), and polymer transcrystallites. The formation of such unique superstructures and organization of the incorporated fillers were realized by a widespread polymer processing technique, wherein a controllable, strong shear flow field was externally applied. The unprecedented reinforcing and toughening effects were achieved for nonfibrous poly(lactic acid) (PLA), one of the most important biodegradable polymers but suffering from limited strength, toughness and heat resistance. The flexibility in the choice of polymer matrices and multifunctional fillers permits broad applications in the fabrication of other specific composites toward low-cost, high-performance, large-scale commodities.

Cite this: DOI: 10.1039/c0xx00000x
www.rsc.org/xxxxxx

COMMUNICATION

Strong and tough micro/nanostructured poly(lactic acid) by mimicking multifunctional hierarchy of shell†

Huan Xu,[‡a] Lan Xie,[‡a] Jing-Bin Chen,[a] Xin Jiang,[a] Benjamin S. Hsiao,[b] Gan-Ji Zhong,*[a] Qiang Fu[a] and Zhong-Ming Li*[a]

Received (in XXX, XXX) Xth XXXXXXXXX 20XX, Accepted Xth XXXXXXXXX 20XX
DOI: 10.1039/b000000x

This effort discloses a bioinspired methodology based on widespread polymer processing techniques for the fabrication of shell-mimicking structural poly(lactic acid) (PLA), one of the most important biodegradable polymers but suffering from limited strength, toughness and heat resistance. The ordered, micro/nanostructural assembly consisting of high-strength phase and tenacious interfacial ligaments was established in the shell-mimicking PLA, by virtue of employing the customized zinc oxide (ZnO) whiskers and intensive shear flow. A demonstration of exceptional properties for the structured PLA was presented, outperforming the normal PLA with a nearly double tensile strength of 119.4 MPa and an over 2.5-fold impact toughness of 11.5 KJ/m^2, as well as the largely enhanced resistance to heat distortion and perfect UV light shielding efficiency. The high strength and toughness are unprecedentedly achieved for PLA, in great need for structural applications.

The past decades have witnessed the revolutionary developments of nanostructured materials to offer unusual properties.[1–7] The important task and competence of developing nanostructured materials is to translate the genuinely amazing properties of individual nanostructures (e.g., nano-sized whiskers, tubes, sheets, etc.) to larger scales.[8–13] Unfortunately, the field of engineered, nanostructured materials is still in its infancy. It is primarily caused by the bottlenecks involving engineering the nanostructures with control, offering materials an incredible range of functional properties, and developing industrial processes for forming the anticipative structures.[14] As a relatively new but rapidly rising star, bionics signifies a promising strategy to build hierarchical constructions, by virtue of mimicking biologically derived materials which carry a special set of properties.[15–19] Biomimetism offers, in principle, the key aspiration to make materials generating structures with true three-dimensional order and multiple contributions to properties in bulk.[20,21] The most famous example is probably the nacreous part of shells, which has been long perceived as rigid biological models for structural composites thanks to their renowned combinations of strength, stiffness and toughness.[22–24] It is essentially a response of three distinguished architectural configurations (Fig. S1 in the Supporting Information): 1) A high volume percentage of multiscale ceramic phase (mainly calcium carbonate, $CaCO_3$) that has shown very high stiffness but limited toughness; 2) The orderly packed layered architecture of the ceramic phase; 3) Thin, tenacious organic components closely connecting the ceramic phase.[25]

Inspired by the biological structural regularities of shells, we attempt to develop shell-mimicking poly(lactic acid) (PLA) composites with the goal of doubling the strength and toughness. Much effort has been devoted to environmentally benign PLA to meet the growing demands of sustainable society, which is ready to show distinct merits including, but not limited to, easy processing, desirable biocompatibility and degradability.[26,27] However, PLA still fails to provide comparable resistance to heat distortion, sufficient ductility and toughness, and adequate strength and stiffness. Consequently PLA has found limited applications in structural materials, and the biomedical fields such as tissue scaffolds and artificial cartilages.[28–30] Hence there is a clear scientific imperative requiring the optimization of the mechanical and thermal performances of PLA.[31–33] Among the traditional approaches to modify PLA, they are formulating and associating with other flexible biopolymers, plasticizers, fibers and nanofillers.[34–37] It appears from the existing literature that performances of these common blending and compositing systems are out of balance. This can be exemplified by the largely sacrificed strength and stiffness after plasticization with poly(butylene succinate),[38] poly[(butylene succinate)-co-adipate][39] or poly(ethylene glycol),[40] and the dwarf of poor ductility and toughness after adding reinforcing elements.[41,42] In sharp contrast, shells are ready to answer the physical demands at extremely high levels, which profoundly relies on the orderly layered multiscale ceramic phase connected by tenacious linkages.[43,44] Is there a way to use bionics as the basis for a new strategy for fabricating PLA structural materials with a hierarchically ordered structure like the shell? Will we encounter more ambitious challenges to develop a practical technology involving the biomimetic process on an industrial scale that is reliable and respects the environment?

To mimic the architectural configurations existing in the shell, assembly of the multiscale components and phases following a clearly defined pattern is of paramount importance to structure PLA. Inorganic zinc oxide (ZnO) whiskers have generated great potential in the structural and biomedical sectors due to their impressive mechanical, optical, catalytical and antimicrobial properties, exciting their established use in health care products and multifunctional fillers with comparably modest cost.[45,46] Particularly customized multiscale ZnO whiskers showing a wide distribution of diameter ranging from several nanometers to tens of micrometer have been chosen to function at both micro- and nano- scales like the multiscale ceramic phase of a shell (Fig. S2). The key challenge is that of orderly organizing these whiskers and structuring tenacious interphase between the whiskers and PLA matrix. Our recent exploration offers the important inspiration that an intense shear flow can preferentially align PLA chains and fibrous fillers, permitting the constructions of smart structure and desirable crystalline morphology.[47,48] In terms of the pivotal role of shear flow, herein we attempt to create shell-mimicking PLA composites introducing micro/nanostructured ZnO whiskers connected by tenacious crystalline superstructures of PLA in the shear. Once such a shell-like multiscale architecture is constructed, an excellent combination of properties is highly prospective.

The shell-mimicking PLA containing 10 wt% ZnO whiskers was structured by melt compounding followed by a modified injection molding, namely oscillation shear injection molding (OSIM). The OSIM technique is characterized by generation of continuous, intense shear flow, as reported elsewhere.[49] Meanwhile, common injection molding (CIM) was also carried out for control purposes. The details of the experimental procedures and the OSIM technique are provided in the Supporting Information.

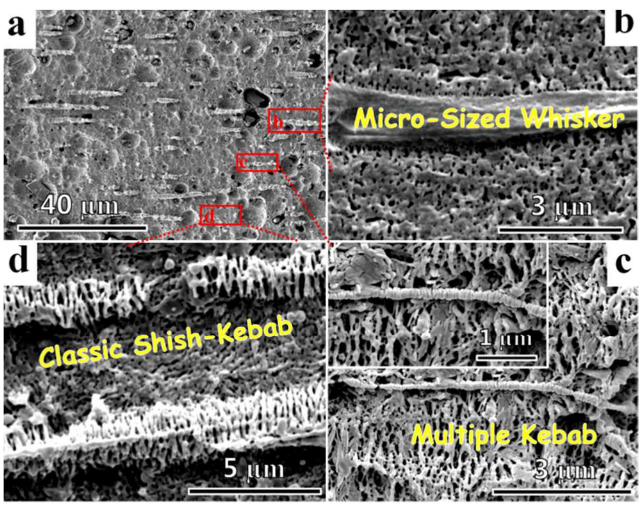

Fig. 1 Scanning electron microscopy (SEM) observations showing the morphology of ZnO whiskers and diverse crystalline superstructures in the oriented layer of the structured PLA. (a) Regularly aligned whiskers along the flow. (b) Typical transcrystallinity developed at a micro-sized ZnO whisker. (c) Multiple kebab structure containing the hybrid shish-kebab induced by a central nanowhisker, and the inset shows the local structure. (d) Classic shish-kebab structure.

The key criteria, verifying the successful creation of shell-mimicking structure, are aligning ZnO whiskers and structuring tenacious interphase between whiskers and PLA matrix (i.e., ordered crystalline entities demonstrating strong interfacial linkage). Fig. 1 offers the direct evidence. Fig. 1a suggests whiskers preferably align along the flow in the structured PLA, in clear contrast to the random distribution in the normal PLA composite (Fig. S6). Obviously, these well-organized whiskers share the same morphological characteristics as the ordered ceramic phase of shell. We further examine the construction of tenacious interfacial crystalline superstructures, mainly regarding the regular arrangement of PLA lamellae at ZnO whiskers as revealed in Fig. 1b and c. Of particular interest are structural features of the tenacious crystalline superstructures that profoundly rely on the whisker size. At the surface of the micro-sized whisker, the typical transcrystallinity is generated to function as the ligament (Fig. 1b). The formation of transcrystallinity stems from the absorption and stabilization of the flow-induced row-nuclei onto the shear-aligned whiskers.[50] For the whiskers whose diameter is of the order of nanometers (the so-called nanowhiskers), they tend to serve as the hybrid shish as illustrated in Fig. 1c. The kebabs induced by the hybrid shish are ready to connect the nanowhiskers closely, and Fig. 1c manifests some unexpected features in the novel hybrid shish-kebab structure of PLA. First, a straight hybrid shish, which has a diameter of about 15 nm, stringing adjacent kebabs, is clearly observed. The hybrid shish presents a length of approximately 6 μm, being entirely decorated with disc-shaped kebabs that are uniform in size and periodically located along the nanowhisker. Second, the entity of hybrid shish-kebab appears to play the role of a "homogeneous fiber", transcrystallizing folded chains which symmetrically develop into the outer kebabs in the columnar appearance.[50] According to the formation order, the kebabs in the inner and outer layers are respectively defined as primary kebabs and secondary kebabs, assembling the multiple kebab structure. This unique hierarchical structure resembles that of cylindrites formed in a flow field.[48,51,52] Third, the primary kebabs are much denser than the secondary lamellae, as evidenced in the inset of Fig. 1c that shows the inner kebabs wrap the nanowhisker with the average periodicity of ~12 nm. In the bulk, Fig. 1d shows the classic shish-kebabs of PLA are formed. The kebabs with a diameter of around 2.1 μm are periodically strung by the central shish into symmetrical cylindrites. As the typical oriented crystalline units, the shish-kebabs developed in PLA demonstrate an important opportunity for improvement of stiffness and strength.[47]

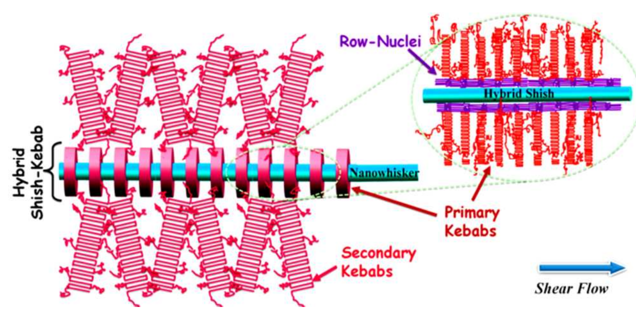

Fig. 2 Schematic representation of the multiple kebab induced by the nanowhisker. The flow direction is horizontal.

Given the above rich oriented crystalline superstructures, the unprecedented observation of the hybrid shish-kebabs containing multiple kebabs prompts our enormous interest, which may play a critical role in mimicking the nacreous structure and shed light on creating tenacious interphase for other nanocomposite systems. To acquire a comprehensive understanding on the formation mechanism of multiple kebabs, the model for this unique structure is schematically depicted in Fig. 2. It consists of a central nanowhisker, flow-induced row-nuclei closely wrapping the whisker, a thin layer of periodically arranged primary kebabs, and a thicker transcrystalline layer of secondary kebabs. The hierarchical structure presumably stems from the different extent of alignment of PLA chains which is a function of the shear rate.[53] The local shear flow is significantly intensified in the vicinity of the nanowhiskers.[54] The nanowhiskers, which present large surface energy, may provide pinning points to the surrounding row-nuclei. Such anchoring interactions can contribute to the retention of the molecular stretch and orientation after flow, which is verified by the melt-crystallization results in Fig. S14. It hence creates more shish structures and promotes the involvement of adjacent chains into multidisc columns of compact primary kebabs embedding in the shish.[55] Secondary kebabs with less lamellar density is elicited when PLA chains are only partially extended, arising from the decreased shear stress level and the disappeared surface anchoring interactions of nanowhisker.[56] The existence of two populations of extended chains also gives rise to the fact that the primary kebabs present an incredibly higher density of active nucleation sites than the secondary kebabs. One may find it instructive to build more tenacious interphase at a higher level of lamellar orientation, motivating further efforts in the performance improvement of PLA products.

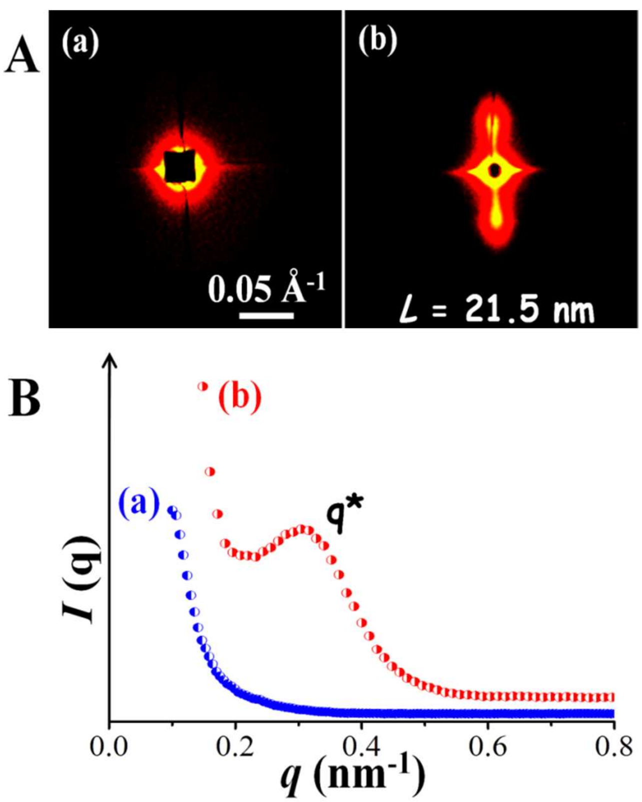

Fig. 3 (A) Representative 2D-SAXS patterns and (B) 1-D SAXS intensity profiles of (a) normal PLA and (b) structured PLA. Oriented shish and lamellae are evidently observed in (b), presenting a long period of 21.5 nm and a lamellar thickness of 10.6 nm.

As a complement for the SEM observation, two-dimensional small-angle X-ray scattering (2D-SAXS) measurements were performed to offer quantitative insights into the tenacious crystalline interphase between ZnO whiskers and PLA matrix for the structured PLA, as shown in Fig. 3. The scattering reflection of oriented crystals is observed exclusively in the structured PLA, displaying a pair of symmetrical triangular streaks in the equatorial direction and a pair of bulb-shape lobes in the meridional direction (Fig. 3A). It apparently manifests the presence of shear-aligned shish and lamellae decorated at the shish and whiskers, well in line with the SEM observations. Fig. 3B illustrates the 1D-SAXS intensity profiles which produce the long period (L) regarding the lamellar structure. We note that the structured PLA presents an L of 21.5 nm, reflecting a statistical averaging outcome for the lamellar spacing in the transcrystallinity and classic shish-kebabs and hybrid shish-kebabs.[48] Furthermore, based on the L and crystallinity (χ_c = 49.2%, Fig. S14), the lamellar thickness (L_t) can be calculated to be 10.6 nm ($L_t = L \times \chi_c$). One may be amazed at the high coincidence between the thickness of oriented lamellae and that of the ultrathin organic layer existing in shell that encases the ceramic component (~10 nm).[22] It is obvious that the construction units of the structured PLA and shell are in the similar size, laying paramount premise to offer multifunction and achieve the shell-mimicking structure.

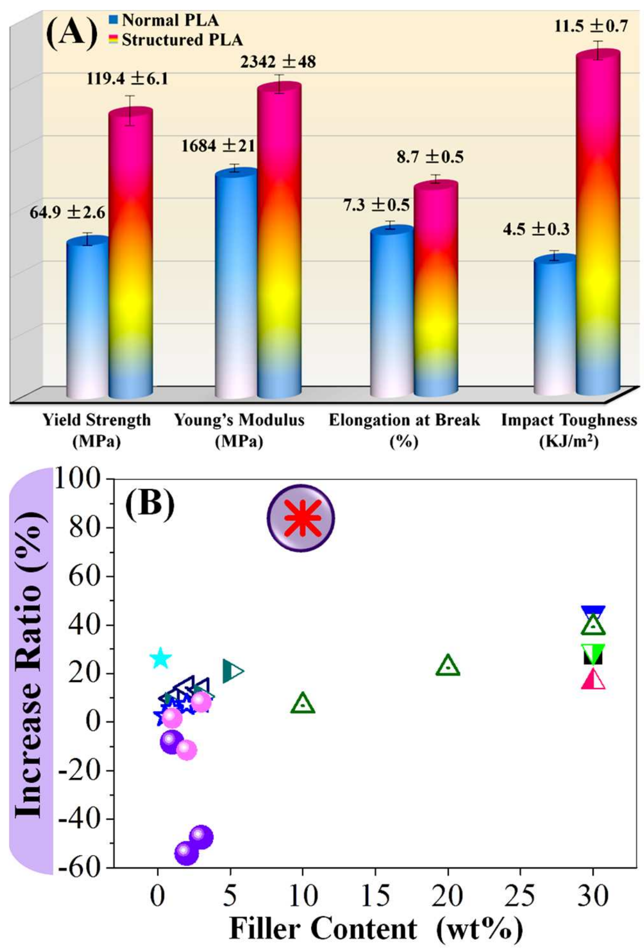

Fig. 4 A series of performance evaluation to demonstrate the exceptional mechanical properties of the structured PLA, as well as the excellent resistance to thermal deformation and specific anti-UV properties. (A) Detailed mechanical results regarding

yield strength, Young's modulus, elongation at break and impact strength. (B) Comparison of increase ratio of tensile strength between (✱) this work and other PLA composite systems based on (■) glass fiber,[57] (▽) man-made cellulose fiber,[58] (▲) abaca fiber,[58] (▼) jute fiber,[58] (△) ramie fiber,[36] (◁) cellulose nanowhisker,[42] (▶) cellulose nanofiber,[59] (☆) multi-walled carbon nanotubes,[60] (★) graphene nanosheets,[61] and (●) untreated and (●) silane treated ZnO,[62] the increase ratio is defined as the increase in tensile strength to the initial value of pure PLA. (a) Normal PLA, (b) structured PLA.

The above results allow to assume that shell-mimicking structural configurations are established in the structured PLA: the oriented whiskers and classic shish-kebabs can be regarded as the rigid ceramic phase, while the interfacial crystalline entities can function as the tenacious linkages like the organic phase of shell. Reasonably, one may expect the exceptional performances of the structured PLA. It is apparent that the unique shell-mimicking structure greatly benefits the mechanical properties of PLA as demonstrated in Fig. 4A. We see from Fig. S15A that, the stress-strain curve of the structured PLA evidently towers over that of the normal PLA. Specifically, compared to the initial values of 64.9 and 1684 MPa of the normal PLA, the structured PLA obtains an unexpected promotion of yield strength and Young's modulus, achieving 119.4 and 2342 MPa, respectively (Fig. 4A). More importantly, the shell-mimicking structure permits the appreciable enhancement of ductility and toughness of the structured PLA, different from the usual sacrifice after incorporating stiff fillers. Particularly, Fig. 4A suggests the elongation at break and resistance to impact of the structured PLA achieve 8.7% and 11.5 KJ/m^2, while the normal PLA shows the values of only 7.3% and 4.5 KJ/m^2, respectively. To clarify the superiority of the shell-mimicking approach over the traditional processing, we have gathered the data regarding the increase ratio of tensile strength in this work and those reported in other PLA composite systems (Fig. 4B). It clearly suggests that the unprecedented optimization of tensile properties has been established under the common industrial processing conditions, while exceptional impact toughness has been simultaneously achieved for the structured PLA.

The unusual combination of mechanical performances suggest interesting generalizations concerning the role of bioinspired structuring in creating evolutionary innovations and adaptive radiation for the manufacture of high-performance PLA. Practically, the traditional systems associated with the normal processing methods (e.g., compression, extrusion, injection molding, and spinning) have unfortunately evolved in fairly unimpressive performances or poor balance of properties. Limited promotion of strength and toughness was observed in the PLA composites and blends, although in those newly developed systems.[63–65] Here the unique shell-mimicking structure advances the strength, stiffness and toughness of PLA simultaneously, which is extremely attractive both academically and commercially.

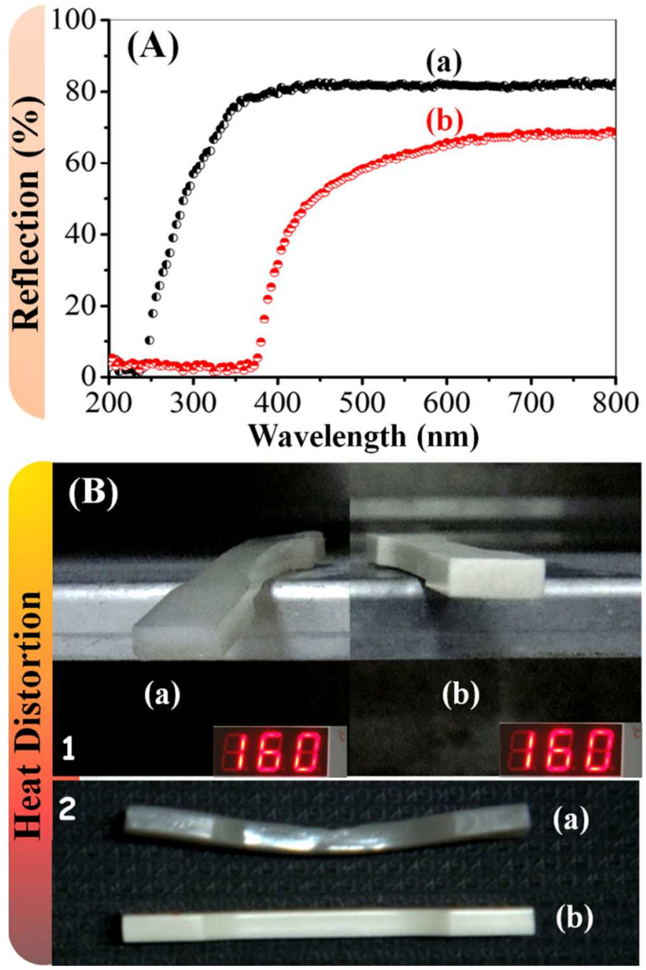

Fig. 5 Excellent resistance to thermal deformation and specific anti-UV properties of the structured PLA. (A) UV-visible reflection spectrum. (B) Digital images indicating the degree of heat deformation after the treatment at 160 °C for 60 min, image 1 shows the frontal appearance of samples in the oven, while image 2 presents the side appearance after cooling down. (a) Normal PLA, (b) structured PLA.

Next, we characterize the large changes in anti-UV property (wavelength between 200 and 400 nm) and heat distortion resistance for the normal PLA and structured PLA, as shown in Fig. 5A and B. Presumably, a very weak UV absorption occurs in the normal PLA. After achieving the shell-mimicking structure, the structured PLA shows almost perfect UV light shielding efficiency. Fig. 5B confirms the strong modification of the heat distortion resistance for the structured PLA by conducting a simple hanging experiment in the oven. The structured PLA sample still preserves the original shape after hanging on the heated steel plate (160 °C) for up to 60 min, while the normal PLA produces destructive heat distortion. These observations emphasize that the design of shell-mimicking structural configurations introduces the capacity to resist loading and deformation occurring at complex circumstances for PLA, especially under environments over 100 °C.[66]

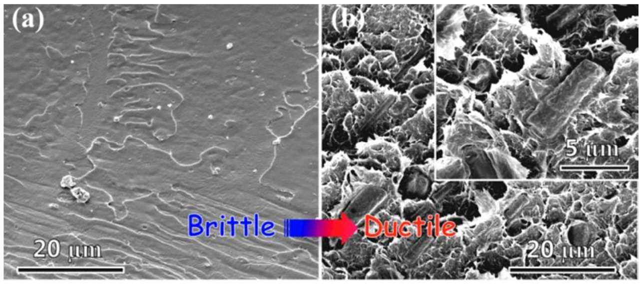

Fig. 6 SEM micrographs of fractured surfaces after tensile failure showing the fundamental transition from the brittle fracture of (a) normal PLA to the ductile fracture of (b) structured PLA.

Recent studies have demonstrated promising application of PLA as an ideal green biopolymer to provide charming renewability, biocompatibility and biodegradability. The manufacture of PLA based structure materials at a reasonable efficiency is an attractive goal, the present effort indicates a satisfactory attempt which will motivate further potential in expanding the application of PLA. One may expect unusual fracture behavior of the structured PLA, judging from the peculiar state of performance beyond an exceptional promotion in strength, stiffness, ductility and toughness. The fracture behaviors of the structured PLA and normal PLA are appraised from the fractured surfaces after tensile failure, as described in Fig. 6. Notably, one clearly observes that some significant changes differentiate the fractured surface of the structured PLA from that of the normal PLA. The fractured surface of the structured PLA is extremely coarse and bumpy with a scale-like appearance (Fig. 6b), which is indicative of plentiful plastic deformation developed during fracture, in sharp contrast to the flat and smooth morphology of the normal PLA without any trace of plastic deformation (Fig. 6a). Such an observation of brittle-to-ductile transition is indeed a remarkable phenomenon that is rarely reported in plasticizer-free PLA composite systems, in favor of dissipating a large amount of energy. It is also worth mentioning that the structured PLA presents substantially enhanced interfacial adhesion as evidenced by the close, tight bonding (Figs. 6b and S17).

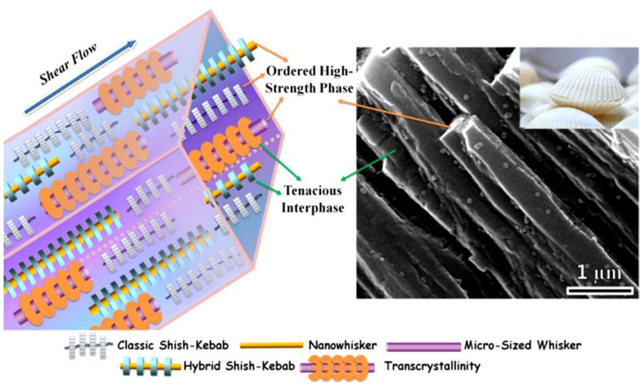

Fig. 7 Schematic diagram comparing the structural features between the structured PLA and shell. Highly oriented micro-sized whiskers and nanowhiskers, and well aligned shish-kebabs in the structured PLA are grouped into ordered high-strength phase like the well-organized multiscale ceramic phase existing in the shell, while transcrystallinity and hybrid shish-kebabs decorating the micro-sized whiskers and nanowhiskers are considered as tenacious interphase like the organic components closely connecting the ceramic phase.

We further attempt to diagram the shell-mimicking features existing in the structured PLA that give rise to the unexpected brittle-to-ductile transition. Fig. 7 extracts the key architectural features shared by the structured PLA and shell, leading to the common definition of two function systems: the ordered high-strength phase and tenacious interphase. It is fairly convinced that such a structured composite system showing extremely basic to the very idea and image of shell is biomimetic in its origins, as specified by Fig. 7. The well aligned shish-kebabs, micro-sized whiskers and nanowhiskers render a multifunctional reinforcement of the PLA matrix. Specifically, the micro-sized whiskers provide excellent mechanical performance of the composite within the plane, while the shish-kebabs and nanowhiskers work at the nanoscale and enhance the through-thickness properties.[67] As for the PLA lamellae arranged at whiskers (i.e., hybrid shish-kebab and transcrystallinity), they are strong as well as resilient and can be regarded as the ligament or filament formation in the interfaces. When encountered the impact deformation, the tight shish-kebabs and whiskers show strong retardation of crack propagation, and cracks are prone to traverse across the thickness of them quite easily rather than the conventional linear development. It ultimately leads to the unusual observation of foliated surface from layer to layer (Fig. 6b). This mechanism can be substantially assisted by the interfacial superstructures, like a kind of sheath, that may construct crack bridging with the dissipation and absorption of much energy.[68] The combination of multiscale reinforcement and strong interfacial bonding desirably permits the effective transfer of applied stress and impact load from layer to layer in the structured PLA, resulting in the brittle-to-ductile transition.[69] In this perspective, we provide the organisms for the structured composite system with shell-mimicking configurations that exhibit impressive combinations of mechanical response. Of paramount significance is the optimized biomimetic solution that will inspire and provide design principles for the rational design and reproducible construction of biobased structural composites with multiscale structures for multifunctional integration.

Conclusions

In the present work, an unprecedented shell-mimicking methodology has been developed for structuring PLA with the goal of doubling the strength and toughness. Particularly, customized multiscale ZnO whiskers were introduced to function at different length scales, while an intensive shear flow was employed during the injection molding to organize the whiskers and to build strong interfacial ligaments. The structured PLA was essentially a direct copy of shell. It was a surprise to find the high coincidence shown in the size of their construction units (~10 nm). Resulting from the shell-mimicking features, the structured PLA yielded high tensile strength and impact toughness (119.4 MPa and 11.5 KJ/m^2), representing specific properties in great need for structural and medical applications. Of particular interest are the largely enhanced resistance to heat distortion and perfect UV light shielding efficiency.

The proposed biomimetic methodology for materials design should be broadly applicable to the industrial manufacturing of various structural polymer composites, because uncontrollable organization of incorporated fillers and poor interfacial bonding are commonly encountered problems in high-performance composite preparation. The key elements in our methodology are the design of multiscale fillers and engineering control of shear flow, which have rarely been studied for structuring polymer composites despite their importance in the practical processing. We anticipate this effort to help advance the structure-by-bionics approach in the fabrication of other composites toward low-cost, high-performance, large-scale commodities.

Acknowledgements

The authors gratefully thank the financial support from the National Natural Science Foundation of China (Grants 51120135002, 51203104 and 51121001), the Innovation Team Program of Science & Technology Department of Sichuan Province (Grant 2013TD0013), the Programme of Introducing Talents of Discipline to Universities (B13040) and the Doctoral Program of the Ministry of Education of China (Grant 20130181130012).

Notes and references

[a] *State Key Laboratory of Polymer Materials Engineering, College of Polymer Science and Engineering, Sichuan University, Chengdu, 610065, Sichuan, People's Republic of China. E-mail: ganji.zhong@scu.edu.cn; zmli@scu.edu.cn*

[b] *Department of Chemistry, Stony Brook University, Stony Brook, New York 11794-3400, United States*

† Electronic Supplementary Information (ESI) available. See DOI: 10.1039/b000000x/

‡ These authors contributed equally to this work.

1 L. Borchardt, M. Oschatz and S. Kaskel, *Mater. Horiz.*, 2014, **1**, 157.

2 A. B. Djurišić, Y. H. Leung and A. M. Ching Ng, *Mater. Horiz.*, 2014, **1**, 400.

3 A. S. Aricò, P. Bruce, B. Scrosati, J.-M. Tarascon and W. Van Schalkwijk, *Nat. Mater.*, 2005, **4**, 366.

4 B. Kolodziejczyk, O. Winther-Jensen, C. H. Ng, S. Lin, Q. Bao and B. Winther-Jensen, *Mater. Horiz.*, 2014, **1**, 452.

5 K. Lee, M. D. Losego, D. H. Kim and G. N. Parsons, *Mater. Horiz.*, 2014, **1**, 419.

6 W. Li, M. Liu, S. Feng, X. Li, J. Wang, D. Shen, Y. Li, Z. Sun, A. A. Elzatahry, H. Lu and D. Zhao, *Mater. Horiz.*, 2014, **1**, 439.

7 Y. Liao, T. P. Farrell, G. R. Guillen, M. Li, J. A. T. Temple, X.-G. Li, E. M. V. Hoek and R. B. Kaner, *Mater. Horiz.*, 2014, **1**, 58.

8 X. Zhang, L. Chen, T. Yuan, H. Huang, Z. Sui, R. Du, X. Li, Y. Lu and Q. Li, *Mater. Horiz.*, 2014, **1**, 232.

9 J. Zhang, J. Wang and H. Tian, *Mater. Horiz.*, 2014, **1**, 169.

10 F.-X. Xiao, J. Miao and B. Liu, *Mater. Horiz.*, 2014, **1**, 259.

11 J. Raeburn, B. Alston, J. Kroeger, T. O. McDonald, J. R. Howse, P. J. Cameron and D. J. Adams, *Mater. Horiz.*, 2014, **1**, 241.

12 R. J. Moerland, J. E. Koskela, A. Kravchenko, M. Simberg, S. van der Vegte, M. Kaivola, A. Priimagi and R. H. A. Ras, *Mater. Horiz.*, 2014, **1**, 74.

13 M. Antonietti, *Nat. Mater.*, 2003, **2**, 9.

14 R. M. Erb, R. Libanori, N. Rothfuchs and A. R. Studart, *Science*, 2012, **335**, 199.

15 C. Sanchez, H. Arribart and M. M. G. Guille, *Nat. Mater.*, 2005, **4**, 277.

16 T. Saito, Y. Oaki, T. Nishimura, A. Isogai and T. Kato, *Mater. Horiz.*, 2014, **1**, 321.

17 K. Liu and L. Jiang, *ACS Nano*, 2011, **5**, 6786.

18 J. Wang, Q. Cheng, L. Lin and L. Jiang, *ACS Nano*, 2014, **8**, 2739.

19 Q. Cheng, M. Li, L. Jiang and Z. Tang, *Adv. Mater.*, 2012, **24**, 1838.

20 H. Yao, G. Zheng, W. Li, M. T. McDowell, Z. Seh, N. Liu, Z. Lu and Y. Cui, *Nano Lett.*, 2013, **13**, 3385.

21 X. Yao, Y. Song and L. Jiang, *Adv. Mater.*, 2011, **23**, 719.

22 G. Mayer, *Science*, 2005, **310**, 1144.

23 Q. Cheng, M. Wu, M. Li, L. Jiang and Z. Tang, *Angew. Chem. Int. Edit.*, 2013, **52**, 3750.

24 Q. Cheng, L. Jiang and Z. Tang, *Accounts Chem. Res.*, 2014, **47**, 1256.

25 J. Wang, Q. Cheng, L. Lin, L. Chen and L. Jiang, *Nanoscale*, 2013, **5**, 6356.

26 L. Xie, H. Xu, Z.-P. Wang, X.-J. Li, J.-B. Chen, Z.-J. Zhang, H.-M. Yin, G.-J. Zhong, J. Lei and Z.-M. Li, *J. Polym. Res.*, 2014, **21**, 357.

27 V. Arias, A. Höglund, K. Odelius and A.-C. Albertsson, *Biomacromolecules*, 2013, **15**, 391.

28 M. Persson, G. S. Lorite, S.-W. Cho, J. Tuukkanen and M. Skrifvars, *ACS Appl. Mater. Interfaces*, 2013, **5**, 6864.

29 S. Van Vlierberghe, P. Dubruel and E. Schacht, *Biomacromolecules*, 2011, **12**, 1387.

30 P. Zhang, H. Wu, H. Wu, Z. Lù, C. Deng, Z. Hong, X. Jing and X. Chen, *Biomacromolecules*, 2011, **12**, 2667.

31 N. Delpouve, G. Stoclet, A. Saiter, E. Dargent and S. Marais, *J. Phys. Chem. B*, 2012, **116**, 4615.

32 J. Sun, H. Yu, X. Zhuang, X. Chen and X. Jing, *J. Phys. Chem. B*, 2011, **115**, 2864.

33 A. J. Svagan, A. Åkesson, M. Cárdenas, S. Bulut, J. C. Knudsen, J. Risbo and D. Plackett, *Biomacromolecules*, 2012, **13**, 397.

34 N. Vasanthan, H. Ly and S. Ghosh, *J. Phys. Chem. B*, 2011, **115**, 9556.

35 F. D'Angelo, I. Armentano, I. Cacciotti, R. Tiribuzi, M. Quattrocelli, C. Del Gaudio, E. Fortunati, E. Saino, A. Caraffa, G. G. Cerulli, L. Visai, J. M. Kenny, M. Sampaolesi, A. Bianco, S. Martino and A. Orlacchio, *Biomacromolecules*, 2012, **13**, 1350.

36 H. Xu, C.-Y. Liu, C. Chen, B. S. Hsiao, G.-J. Zhong and Z.-M. Li, *Biopolymers*, 2012, **97**, 825.

37 N. Lavielle, A. Hébraud, G. Schlatter, L. Thöny-Meyer, R. M. Rossi and A.-M. Popa, *ACS Appl. Mater. Interfaces*, 2013, **5**, 10090.

38 K. Zhang, A. K. Mohanty and M. Misra, *ACS Appl. Mater. Interfaces*, 2012, **4**, 3091.

39 V. Ojijo, S. Sinha Ray and R. Sadiku, *ACS Appl. Mater. Interfaces*, 2012, **4**, 6690.

40 Z. Kulinski, E. Piorkowska, K. Gadzinowska and M. Stasiak, *Biomacromolecules*, 2006, **7**, 2128.

41 C. Zhou, Q. Shi, W. Guo, L. Terrell, A. T. Qureshi, D. J. Hayes and Q. Wu, *ACS Appl. Mater. Interfaces*, 2013, **5**, 3847.

42 M. Martínez-Sanz, A. Lopez-Rubio and J. M. Lagaron, *Biomacromolecules*, 2012, **13**, 3887.

43 F. Bouville, E. Maire, S. Meille, B. Van de Moortèle, A. J. Stevenson and S. Deville, *Nat. Mater.*, 2014, **13**, 508.

44 M. A. Meyers, J. McKittrick and P. Y. Chen, *Science*, 2013, **339**, 773.

45 V. B. Schwartz, F. Thétiot, S. Ritz, S. Pütz, L. Choritz, A. Lappas, R. Förch, K. Landfester and U. Jonas, *Adv. Funct. Mater.*, 2012, **22**, 2376.

46 X. Zhou, T. Lin, Y. Liu, C. Wu, X. Zeng, D. Jiang, Y.-a. Zhang and T. Guo, *ACS Appl. Mater. Interfaces*, 2013, **5**, 10067.

47 H. Xu, G.-J. Zhong, Q. Fu, J. Lei, W. Jiang, B. S. Hsiao and Z.-M. Li, *ACS Appl. Mater. Interfaces*, 2012, **4**, 6774.

48 H. Xu, L. Xie, Y.-H. Chen, H.-D. Huang, J.-Z. Xu, G.-J. Zhong, B. S. Hsiao and Z.-M. Li, *ACS Sustainable Chem. Eng.*, 2013, **1**, 1619.

49 Y.-H. Chen, G.-J. Zhong, Y. Wang, Z.-M. Li and L. Li, *Macromolecules*, 2009, **42**, 4343.

50 H. Xu, L. Xie, X. Jiang, X.-J. Li, Y. Li, Z.-J. Zhang, G.-J. Zhong and Z.-M. Li, *J. Phys. Chem. B*, 2013, **118**, 812.

51 B. Larin, C. A. Avila-Orta, R. H. Somani, B. S. Hsiao and G. Marom, *Polymer*, 2008, **49**, 295.

52 H. Xu, L. Xie, X. Jiang, M. Hakkarainen, J.-B. Chen, G.-J. Zhong and Z.-M. Li, *Biomacromolecules*, 2014, **15**, 1676.

53 H. Fang, Y. Zhang, J. Bai and Z. Wang, *Macromolecules*, 2013, **46**, 6555.

54 A. Jabbarzadeh and R. I. Tanner, *Macromolecules*, 2010, **43**, 8136.

55 B. Shen, Y. Liang, C. Zhang and C. C. Han, *Macromolecules*, 2011, **44**, 6919.

56 F. Zuo, J. K. Keum, L. Yang, R. H. Somani and B. S. Hsiao, *Macromolecules*, 2006, **39**, 2209.

57 M. Huda, L. Drzal, A. Mohanty and M. Misra, *Compos. Sci. Technol.*, 2006, **66**, 1813.

58 A. K. Bledzki and A. Jaszkiewicz, *Compos. Sci. Technol.*, 2010, **70**, 1687.

59 M. Jonoobi, J. Harun, A. P. Mathew and K. Oksman, *Compos. Sci. Technol.*, 2010, **70**, 1742.

60 C.-S. Wu and H.-T. Liao, *Polymer*, 2007, **48**, 4449.

61 Y. Cao, J. Feng and P. Wu, *Carbon*, 2010, **48**, 3834.

62 M. Murariu, A. Doumbia, L. Bonnaud, A. L. Dechief, Y. Paint, M. Ferreira, C. Campagne, E. Devaux and P. Dubois, *Biomacromolecules*, 2011, **12**, 1762.

63 R. N. Darie, E. Pâslaru, A. Sdrobis, G. M. Pricope, G. E. Hitruc, A. Poiată, A. Baklavaridis and C. Vasile, *Ind. Eng. Chem. Res.*, 2014, **53**, 7877.

64 K. M. Z. Hossain, M. S. Hasan, D. Boyd, C. D. Rudd, I. Ahmed and W. Thielemans, *Biomacromolecules*, 2014, **15**, 1498.

65 H. Zhao, Z. Cui, X. Sun, L.-S. Turng and X. Peng, *Ind. Eng. Chem. Res.*, 2013, **52**, 2569.

66 X. Zhang, R. Nakagawa, K. H. K. Chan and M. Kotaki, *Macromolecules*, 2012, **45**, 5494.

67 E. Bekyarova, E. T. Thostenson, A. Yu, M. E. Itkis, D. Fakhrutdinov, T.-W. Chou and R. C. Haddon, *J. Phys. Chem. C*, 2007, **111**, 17865.

68 S. Kamat, X. Su, R. Ballarini and A. Heuer, *Nature*, 2000, **405**, 1036.

69 E. Bekyarova, E. Thostenson, A. Yu, H. Kim, J. Gao, J. Tang, H. Hahn, T.-W. Chou, M. Itkis and R. Haddon, *Langmuir*, 2007, **23**, 3970.

Table of Contents Entry

Strong and Tough Micro/Nanostructured Poly(lactic acid) by Mimicking Multifunctional Hierarchy of Shell

Huan Xu,[‡a] Lan Xie,[‡a] Jing-Bin Chen,[a] Xin Jiang,[a]

Benjamin S. Hsiao,[b] Gan-Ji Zhong,*[a] Qiang Fu[a] and Zhong-Ming Li*[a]

[a] State Key Laboratory of Polymer Materials Engineering, College of Polymer Science and Engineering, Sichuan University, Chengdu, 610065, Sichuan, People's Republic of China

[b] Department of Chemistry, Stony Brook University, Stony Brook, New York 11794-3400, United States

[‡] These authors contributed equally to this work.

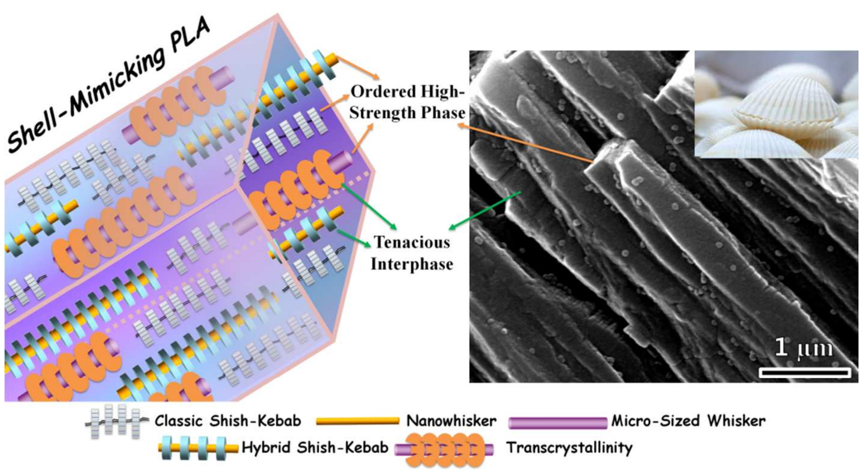

The present work discloses a bioinspired methodology for the unprecedented achievement of simultaneously strong, tough and stiff PLA.